PROCEEDINGS, Thirty-Sixth Workshop on Geothermal Reservoir Engineering
Stanford University, Stanford, California, January 31 - February 2, 2011
SGP-TR-191

HEAT FLUX FROM STEAMING GROUND: REDUCING UNCERTAINTIES

Chris J. Bromley[1], Saskia M. van Manen[1], Warren Mannington[2]

[1]GNS Science, Private Bag 2000
[2] Contact Energy, Private Bag 2001
Wairakei, Taupo, 3352, New Zealand
e-mail: c.bromley@gns.cri.nz

ABSTRACT

Improved calibration of geothermal reservoir models can be achieved with more accurate input data, including assessments of surface heat loss from areas of naturally steam-heated ground. In the past, these have proven to be notoriously difficult to assess, with large uncertainties leading to poor knowledge of changes in surface heat flux values. Using a 2009-2010 comprehensive study of heat flux from the Tauhara sector of the Wairakei-Tauhara system as a case study, this paper discusses three new practical methods and a theoretical approach, which reduce the uncertainties in such assessments. This has implications for improved monitoring of heat flux values in similar settings, and therefore improved predictive capabilities of future reservoir simulations. The total heat loss from surface thermal features in 2010 at Tauhara was assessed to be 86 (+/- 10) MW (thermal), similar to the 1950's pre-Wairakei assessment of heat loss from the same area of about 100 MW, and significantly less than the 1970's assessment of about 220 MW. A higher proportion (63%) now originates from areas of steaming ground compared to discharging hot springs.

INTRODUCTION

Steaming ground is a thermal manifestation that results from vapour that rises to the surface above boiling liquid- and vapour- dominated geothermal systems and hydrothermal volcanic reservoirs. Heat transfer occurs by conduction, convection and radiation. Conduction occurs in a thin near-surface layer with a steep temperature gradient that is often maintained by subsurface convection ('heat-pipe' mechanism). Surface convection predominantly occurs from direct discharge through cracks, vents and fumaroles, along with diffuse discharge of steam through the soil. Radiation is emitted from the heated ground surface. Surface heat flux estimates provide constraints for calibration of geothermal reservoir models, and as these models become more refined, more accurate assessments of surface heat flux are required. In addition, increased awareness of environmental changes associated with the extraction of fluids from geothermal reservoirs has led to an increased need to monitor surface heat flux. Assessing heat flux from large areas of steaming and conductively-heated ground is a particularly difficult task because of the variability of key parameters with time, sensitivity to atmospheric conditions (such as pressure, ambient temperature and rainfall), and the diversity of interacting heat transfer processes. In this setting, shallow heat conduction may actually contribute just a small proportion of the total surface heat flux. Here we present and contrast four different methods of assessing heat flux from steaming ground, illustrated by a case study from the Tauhara sector of the Wairakei-Tauhara geothermal system, Taupo, New Zealand. Three of the methods for determining heat flux from steam-heated ground have been adapted from the techniques previously developed. The fourth method uses a theoretical approach based solely on surface thermal radiation. We also touch upon heat flux from springs, seeps and hydrothermal eruption craters, as these contribute to the overall surface heat flux. But because they are subject to different sources of uncertainty, we do not discuss them here in detail.

BACKGROUND

Heat flux through areas of steaming ground in New Zealand (Wairakei-Tauhara) was first assessed by Banwell et al. (1957). Further studies were published by Benseman (1959), Thompson et al. (1964) and Dawson (1964), and the methods presented in those were used until the late 1990s. Mongillo and Graham (1999) investigated a relationship between Thermal Infrared (TIR) derived surface temperature and heat flux for night time conditions. Using shallow temperature gradients and an assumed thermal conductivity they established the following empirical relationship for a 5 ha study site in the Crown Road thermal area of Tauhara:

$$Q = a(T_s - T_{amb}) \qquad \text{(Eq. 1)}$$

where Q is in Wm^{-2}, a = 27.5 *(empirically derived constant)*, T_s is the surface temperature and T_{amb} is the ambient temperature. Allis et al (1999) calculated heat flux estimates for the Wairakei and Dixie Valley (USA) geothermal systems based on TIR survey. They found a value of 7 for a, and their T_s value is taken at 1 cm depth. The most recent advances in experimental methods to quantify surface heat flux are based on a series of measurements at Karapiti ('Craters of the Moon', Taupo, New Zealand) and on a small area of steaming bare ground near borehole TH1 at Tauhara (Bromley and Hochstein, 2000, 2005; Hochstein and Bromley, 2001, 2005). Hochstein and Bromley (2005) determined an empirical formula to calculate boiling point depths (z_{BP}) based on temperature-depth profiles :

$$z_{BP} = \exp[c_1(T_{BP} - T_Z)] + c_2 \qquad \text{(Eq. 2)}$$

where T_z is the temperature recorded at depth z, c_1 and c_2 are constants (c_1 = -0.025 and c_2 is a fitted site specific factor), T_{BP} is the boiling point temperature (98.6°C in the Tauhara area for average atmospheric pressure). Once z_{BP} is known, total heat flux (Q_{tot}) at that depth is calculated using the following empirical function (Hochstein & Bromley, 2005):

$$Q_{tot} = a\left(\frac{z_{BP}}{z_0}\right)^{-b} \qquad \text{(Eq. 3)}$$

where a = 185 Wm^{-2} (*empirically derived constant*), Z_0 =1 m (normalised), and b = 0.757.

Tauhara

The Tauhara geothermal field (Figure 1) is connected to the Wairakei field, which has been in production since 1958. The pre-development heat loss at Tauhara is estimated to have been 100 (± 20) MW (Hunt et al., 2009). Fisher (1965) published values of about 97 MW for the period 1958-65, and 107 MW from 1951-1952 data, using information from Gregg (1958). The pre-development heat loss of 100 MW is also consistent with estimates by Ellis and Wilson (1955) from Waikato River chloride flux measurements. Due to subsurface boiling induced by Wairakei reservoir pressure decline, a steam-driven heat pulse occurred at Tauhara between about 1965 and 1980, and this caused an increase in heat discharges from steam-heated ground (with an associated decrease from chloride hot springs). A peak value of approximately 217 (± 40) MW surface heat discharge was reached in the 1970s, after which declining steam pressures and declining temperatures of steam-heated groundwater saw the heat discharge rate drop (Allis, 1981, DSIR, 1988).

DATA COLLECTION

To provide information to support a new assessment of Tauhara heat-flux, ground temperature measurements were made during December 2009 and January 2010 at more than 100 representative sites across Tauhara thermal ground areas, and where possible at three depths: 15, 50 and 100 cm (Figure 1). Aerial TIR data were collected March 15-21, 2009 using a helicopter mounted FLIR (Forward Looking Infrared Radiometer) P640 camera. The FLIR consists of an uncooled microbolometer, which uses an array of 640×480 individual sensor elements to detect radiation at wavelengths between 7.5-13 μm. At the flight height of 750 m this results in each image covering ~7.7 ha, and each pixel represents 0.25 m^2 (Figure 2). Atmospheric temperatures and relative humidity at these times were obtained from a NIWA (National Institute of Water & Atmospheric research) station located at the Taupo airport. These enabled processing of the FLIR data using appropriate parameters and provided ambient air temperature values. Hot water streams and springs were also flow-gauged and temperatures recorded of pools, springs and seeps in order to assess heat loss from these thermal features.

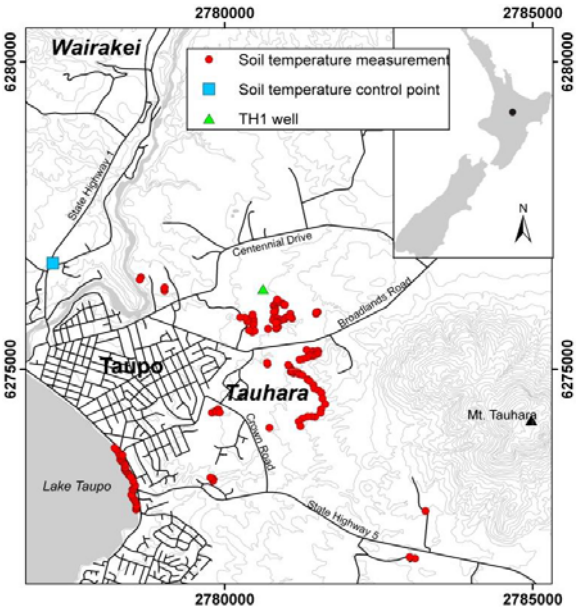

Figure 1. Location map of the Tauhara and Wairakei fields. Red dots are soil temperature sites, blue square is the soil temperature control point and the green triangle is well TH1.

METHODS

Four different methods were used to determine heat flux from steaming ground in the Tauhara area. The first two rely on determining the distribution of boiling point depths (z_{BP}), while the third and fourth methods take an empirical and theoretical approach respectively to calculate heat flux from the surface temperature distribution directly.

1. Heat flux from ground-based temperature measurements

The temperature profiles obtained throughout the Tauhara area, in the summer of early 2010, were used to calculate boiling point depths (z_{BP}) using equation 2. Boiling point depths were divided into three groups: (1) sites where z_{BP} < 1 m, these are generally located on bare ground, (2) areas where 1 m< z_{BP} <25 m, these are typically covered in thermotolerant vegetation (predominantly *Kunzea ericoides* var. *microflora*, commonly known as prostrate kanuka, up to 1.5m high) and (3) areas with 25 m< z_{BP} <35 m, these are covered in thermotolerant vegetation >1.5 m as the surface temperature in these areas is only a few degrees above ambient temperature.

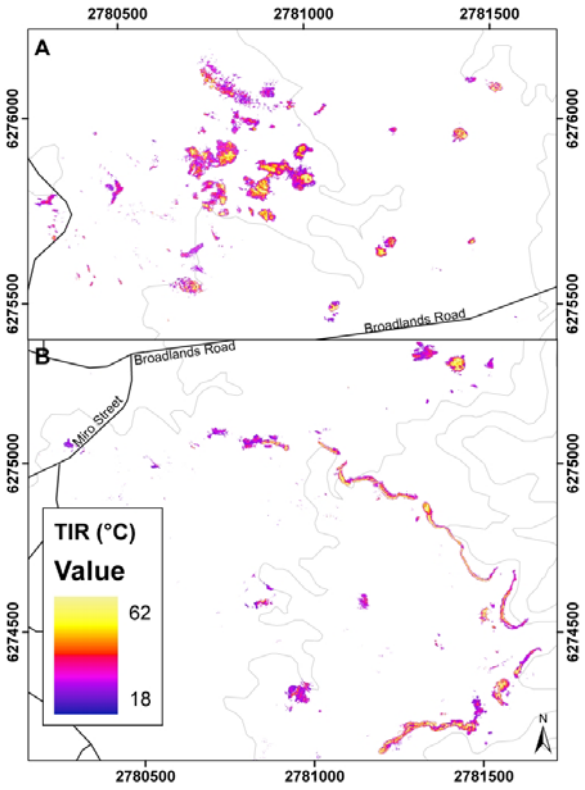

Figure 2. Central Tauhara thermal infrared data (T >18°C) on 20m spaced topographic contour base-maps: (A) Broadlands Road Scenic Reserve; (B) Crown Road area.

Distribution of boiling point depths was then determined by using a contour plot of surface temperature derived from geo-referenced mosaics of TIR data in conjunction with polygon tracing off recent aerial photographs to determine the extent of the thermally anomalous areas. Bare thermal ground occupies ~7 ha, while thermotolerant vegetation <1.5 m covers ~24 ha and the extent of areas with thermotolerant vegetation >1.5 m is ~19 ha. The sum of these three categories of thermal ground (50 ha) approximately matches the independently assessed sum of the Tauhara areas of prostrate-kanuka thermal vegetation and bare ground (50.5 ha, Wildlands, 2004). Histograms of the relative distribution of z_{BP} into 0.1, 1.0 or 5m depth intervals were separately determined for bare ground (z_{BP}<1m) and vegetation-covered thermally anomalous areas (Figure 3). This process enabled the total areas of thermally anomalous ground to be subdivided into areas of equivalent heat flux. These subdivided areas were then multiplied by their average heat flux values, as determined using Equation 3, from the boiling-point depth for the mid-point of each temperature interval. Summing these results provides a value for the total heat flux from steam-heated areas at Tauhara.

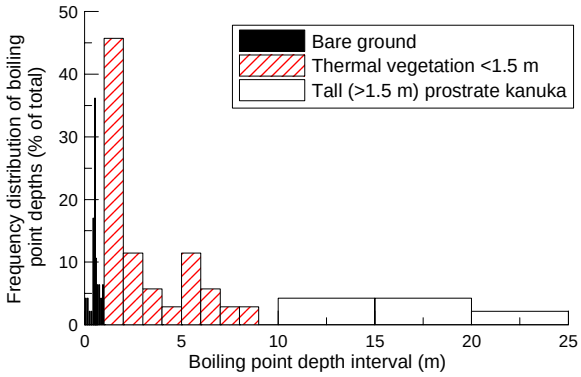

Figure 3. Combined histograms across two ranges of boiling point depths (<or>1m) calculated from temperature profiles in Tauhara hot areas. The width of the bars relates to the width of the depth interval.

2. Indirect calculation of heat flux from the TIR temperature distribution

The second method makes use of the distribution of apparent IR ground surface temperatures across the steam-heated ground. The first step is to combine the histogram distributions of surface temperature from separate TIR images. Figure 4, based on 16 images, shows, as expected, that the maximum numbers of pixels occur in the near-ambient ground temperature range (10 $\pm$ 2°C). The lower than ambient temperatures are believed to be due to low emissivity steel roofs that occur within a particular image.

For ground conditions where the IR surface temperature is more than 15°C (i.e. >5°C above ambient) the distribution of ground temperatures with respect to normalised area (relative to the total area covered by the 16 images, 122.9 ha) can be described using two exponential functions (Figure 5):

$y = 0.263e^{-0.163x}$ for 15<x<48°C, R^2=0.997 (Eq. 4)

$y = 224e^{-0.302x}$ for 48<x<67°C, R^2=0.989 (Eq. 5)

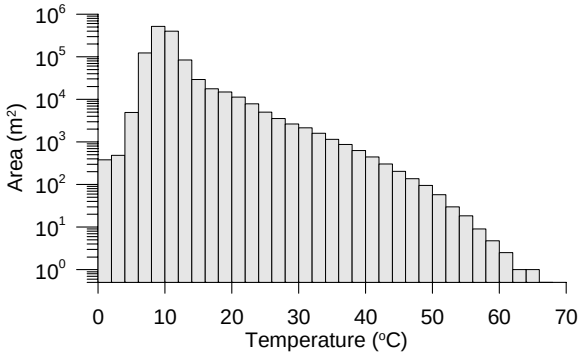

Figure 4. Area per 2°C temperature interval from 16 IR images of steam-heated ground at Tauhara, assuming each pixel represents 0.25 m^2.

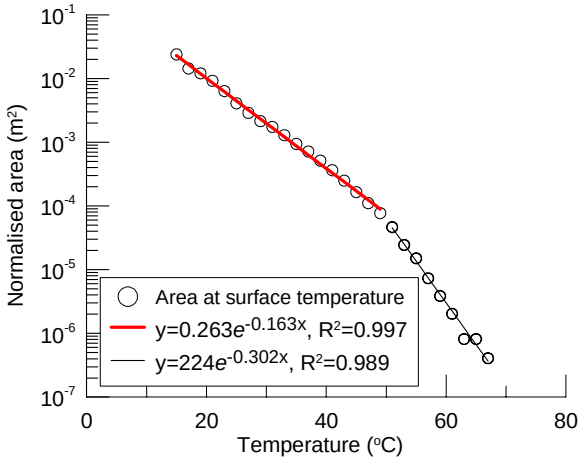

Figure 5. Fitted exponential decay curves to the surface temperature distribution in Figure 4. The change in gradient at 48°C is due to absorption of IR radiation by steam.

The summed area of apparent ground temperature between 48°C and 67°C based on the IR data amounts to 220 m^2, which approximately represents the total area of vigorously steaming ground. Therefore the change in gradient at 48°C is a consequence of concentrated steam emission which partially absorbs infrared radiation, thereby masking the true ground temperature at these sites.

The second step is to calculate z_{BP} for the midpoint of each surface temperature interval. This was achieved in two parts. The first using an empirical formula (Equation 6) relating average boiling point depth to average surface temperature (T_s) minus ambient air temperature (T_{amb}) based on statistical treatment of a 2 year set of monitoring data near borehole TH1 where the boiling point depth ranged from 1 - 5 m depth (Figure 6):

$$z_{BP} = 63.5e^{-0.715(T_s - T_{amb})} \qquad \text{(Eq. 6)}$$

for z_{BP} > 1 m, R^2 = 0.99. The second part of the formula applies to shallower boiling point depths (< 1 m, mostly consisting of bare or moss-covered ground) and uses Equation 7, based on a best-fit empirical function, as illustrated in Figure 7, for summer data from 30 sites at Karapiti and Tauhara.

$$z_{BP} = 5.26(T_s - T_{amb} - 2.5)^{1.3} \qquad \text{(Eq. 7)}$$

for z_{BP} <1 m, R^2 = 0.96. The third step is to calculate the average heat-loss for each temperature interval using Equation 3, and then multiply the area within each interval by its average heat-loss and sum to determine the total.

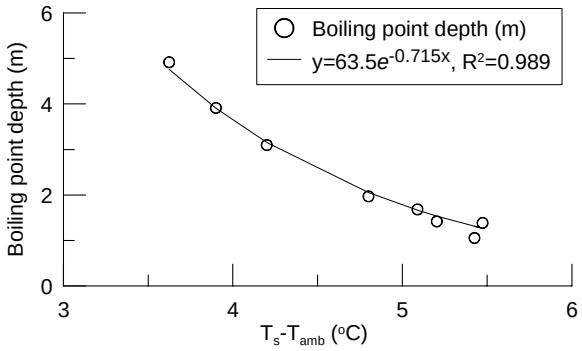

Figure 6. Boiling point depth (m) versus temperature difference (surface-ambient) in °C from average over 2 years (5 am daily data) at 7 warm sites near TH1. Line shows best-fit correlation curve (1-5m z_{BP}).

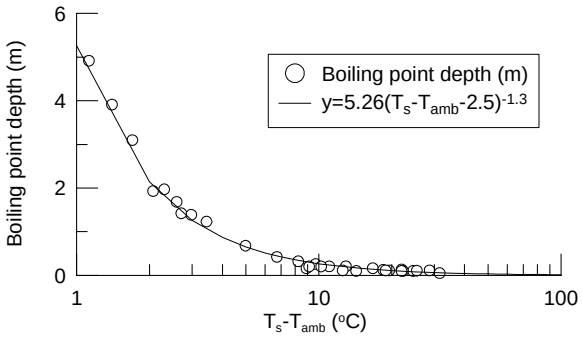

Figure 7. Combined plot of boiling point depth (m) versus log temperature difference (surface -ambient-2.5 °C), with spot data from 30 hotter ground sites at Karapiti/Tauhara. Line shows best-fit correlation (0-5m z_{BP}).

3. Direct calculation of heat flux from the TIR temperature distribution

This method is similar to the one described above, but in this case heat flux (Q_{tot}) for each temperature interval is calculated directly from the difference between T_s and T_{amb} using the following empirical correlation functions (Figure 8):

$$Q_{tot} = 50.3(T_s - T_{amb}) - 148 \qquad \text{(Eq. 8)}$$

for z_{BP} < 1 m, R^2 = 0.73

$$Q_{tot} = 20(T_s - T_{amb}) \quad \text{(Eq. 9)}$$

for $z_{BP} > 1$ m, $R^2 = 0.56$.

Figure 8 illustrates the correlation used in Equation 8. Equation 9 is a best fit linear trend based on conductive heat loss measurements for sites where the surface temperature anomaly is relatively low (<5°C above ambient) and where boiling point depths are greater than 1 m. It compares favourably (within uncertainties) with equation 1.

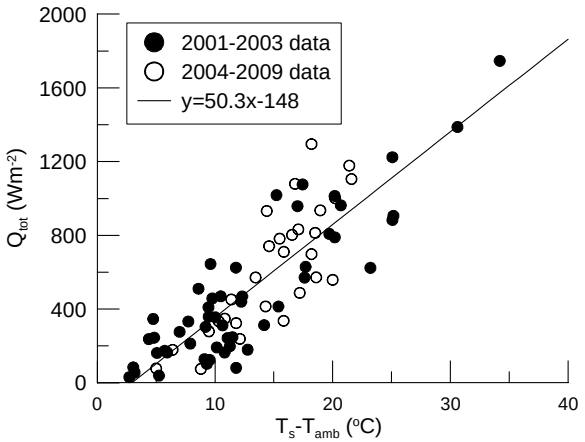

Figure 8. Heat flux on the ground surface versus the temperature difference (surface-ambient). Line shows best-fit correlation curve based on all data from Karapiti and Tauhara calorimeter sites 2001-2009.

The calculated heat fluxes are then multiplied by the respective areas (based on the frequency distribution of pixel temperatures from 16 combined IR images) for each temperature interval, and summed to determine the total.

4. Theoretical heat flux from TIR data

For comparison purposes, heat flux from anomalously hot areas was calculated using a fourth method, which used a subset of the FLIR data that defined anomalously hot ground as > 18°C (Figure 2). Theoretical radiative heat flux (Q_r), convective (Q_c) and conductive (Q_k) fluxes from anomalously hot ground to the air were calculated as follows:

$$Q_r = \tau\sigma\varepsilon A\left(T_s^4 - T_{amb}^4\right) \quad \text{(Eq. 10)}$$

$$Q_c = h_c A\left(T_s - T_{amb}\right) \quad \text{(Eq. 11)}$$

$$Q_k = kA\left(T_s - T_{amb}\right) \quad \text{(Eq. 12)}$$

where τ is the atmospheric transmissivity, σ is the Stefan-Boltzmann constant (5.6704×10^{-8} $Wm^{-2}K^{-4}$), ε is the emissivity (for ground ε = 0.96), A is the surface area at T_s, T_s is the surface temperature of the hot ground (in K= 273.15 +T (°C)), T_{amb} is the background ambient air temperature, h_c is the convective heat transfer coefficient of air (11 W m^{-2} K^{-1}) (Keszthelyi and Denlinger, 1996) and k is the thermal conductivity of air (0.024 W m^{-1} K^{-1}). Atmospheric transmissivity (τ) for infrared radiation is also difficult to account for accurately as it is affected by the transmissivity of the air column between the IR instrument and the ground, including the effect of gases (such as steam), which can be variable. For simplicity, a transmissivity of 1 has been assumed, but it should be recognised that areas of significant steam emission or fog accumulation will have much lower atmospheric transmissivities. Ambient background air temperature during the FLIR survey varied with time, but the average was 12°C based on air temperature records at Taupo airport.

Heat flux from springs, seeps and hydrothermal eruption craters

Heat flux from the two main springs in the Tauhara area was determined using:

$$q_{spring} = (h_{source} - h_{ambient})\dot{m} \quad \text{(Eq. 12)}$$

where h is specific enthalpy and $\dot{m}$ is the mass flow rate of the stream. Heat flux from hot water seepage along the edges of Lake Taupo has also been calculated using Equation 12. Heat flux from hydrothermal eruption craters in the Broadlands Road Reserve was obtained using:

$$Q_{evap} = A \times \Delta H \quad \text{(Eq. 13)}$$

where A is the surface area of the crater and ΔH is the experimentally determined heat loss from a calm surface in kW m^{-2} as a function of temperature, assuming wind speed is zero (Dawson, 1964).

RESULTS

Table 1 outlines the results of the four methods for steam-heated ground. Not all methods were applied to the same datasets, so in order to assist with method comparisons, the results have been subdivided according to the input parameters. To compare the results from the theoretical approach (Method 4) with the direct and indirect methods (2 and 3) from the TIR temperature distribution, these latter methods were re-applied to a subset of data, for T>18°C. A third category (z_{BP} < 0.1 m) was also added for Method 1, as the high surface temperatures associated with this category are not observed in the TIR data due to its spatial resolution. This value (5.3 MW) agrees well with the difference observed in total heat flux between Method 1 and the direct and indirect TIR based methods (2 and 3). The T_s>48°C category has been added to demonstrate the result of the change in gradient (Figure 5) associated with attenuation of the IR radiance due to steam. The effect is demonstrated by the relatively low calculated value (0.43 MW) for this category of high temperature ground when using Methods 2 and 3.

The calculated heat flux values using the direct and indirect methods from the TIR temperature distribution as applied to 2°C intervals are shown in Figure 9. Results from both methods are similar, but the direct method shows slightly greater conductive heat flux from lower temperature thermal ground, and slightly less from hotter ground. Heat flux from springs, seeps and craters is outlined in Table 2.

Table 1. Heat flux in MW through steam-heated ground at Tauhara.

Method	Q $T>T_{amb}$	Q T>18°C	Q $z_{BP}<0.1$m	Q $T_s>48$°C
1	50.8		5.3	
2	46.7	35.6		0.43
3	47.7	33.4		0.43
4		32.4		

Table 2. Heat flux from springs, seeps and craters.

Source	Q (MW)
Hydrothermal eruption craters	3.7
Hot Springs	25.6
Seeps & springs along Lake Taupo edge	6.1
Estimate of minor steam vents	4

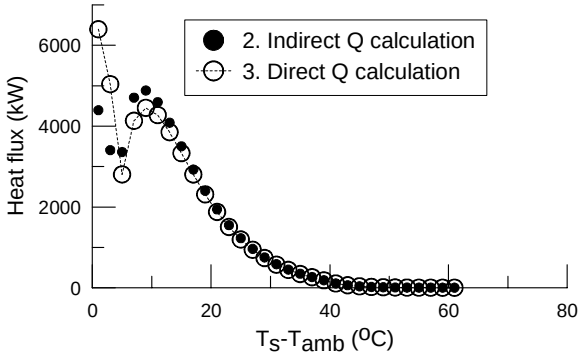

Figure 9. Results from indirect (2) and direct (3) heat flux calculations per temperature interval based on TIR temperature distributions.

DISCUSSION

For steam-heated ground, Table 1 shows consistent total values for Methods 1 to 3 (within 10%) and consistent partial values (*T*>18°C) for Methods 2 to 4. The heat-flux from vigorously steaming areas is likely to be under-estimated using TIR-based Methods 2 to 4 because of the effect of infrared radiation absorption by steam (causing low atmospheric transmissivity). Although some smoothing is inevitable, even with pixel sizes of 0.25 m^2, the TIR imagery is superior in terms of statistically valid distributions of thermally anomalous ground, compared to Method 1, which suffers from insufficient data points, and the possibility of non-random distribution of the locations of the temperature/depth profiles, leading to a possible bias in the data-set when used to create distribution functions of areas within particular temperature ranges. However, for the direct, indirect and theoretical approaches, it is also important to note that the FLIR data (which was collected at night in late summer, March 2009) consists of an average of surface temperature across a 0.25 m^2 pixel, potentially under-representing smaller sources of heat flux such as steam vents. A further uncertainty stems from the potential of thick prostrate kanuka vegetation and steam to obscure or attenuate the thermal infrared signal. For thickly vegetated thermal ground, several conditions such as leaf moisture content and percentage of ground cover will cause the observed TIR temperature to differ from ground surface temperature. The best results can be expected for intermediate ground temperatures associated with low level vegetation and bare ground not vigorously steaming (such as about 18 °C to 48 °C). The indirect method of calculating heat flux from TIR surface temperature distributions is preferable over the direct method based on the robustness of the correlation functions. Method 4 is perhaps the easiest to adopt for future repeat surveys, but it can under-represent the total heat flux if the cut-off temperature is too high.

A total heat flux of 86 (± 10)* MW is obtained based on the indirect method of calculating heat flux from TIR surface temperature distributions for steaming ground, an estimate of discharge from numerous minor steam vents, and calculated heat-flux from hot pools (located in eruption craters), hot springs and seeps. The total value is likely to be a minimum as possible heat flux through the bed of Lake Taupo from a suspected but undetected subsurface hot water outflow has not been included, nor has conductive heat loss outside the main areas of thermally anomalous ground, and nor have discharges from most shallow domestic and commercial bores. In addition, heat loss from small discreet steam vents is difficult to measure, and although estimated, may not have been fully accounted for.

* Uncertainty in total heat flux (+/-12%) was assessed by combining the relative contributions from each of the summed components, based on assessed measurement errors, consistency between alternative methods, and sampling uncertainty due to natural, temporal and geographic variability. The component uncertainties are as follows: +/-50% for minor steam vents, +/-20% for lake edge seeps, and +/- 10% for the remaining components.

CONCLUSIONS

Heat flux estimates from the Tauhara area for 2009-2010 result in an average value of 86 (± 10) MW, of which 63% originates from steaming ground. Studies such as these can provide improved constraints for numerical reservoir simulation models such as the

TOUGH2 model of Wairakei-Tauhara by O'Sullivan and Yeh (2010). Depending on various future production-injection scenarios, their model predicts a decrease in natural surface heat flux at Tauhara to 50 MW, about half of its current value, by 2020 (due to a continuing decline in natural steam flux), after which it increases to between 70 MW and 110 MW by 2060 (due to an increase in hot liquid discharge from existing vents located near the injection area). The 2009/2010 heat flux value obtained for the Tauhara area of 86 MW is similar to that predicted by the current version of the model (100 MW), although the history match is not yet optimized. The detail contained within these new estimates should lead to improved calibration of future versions of the geothermal reservoir model, and therefore improved predictive capabilities of future reservoir simulations.

ACKNOWLEDGEMENTS

The authors would like to thank Contact Energy for permission to use the data in this paper. Romy Bromley assisted with data collection and processing, and Erin Wallin processed the infrared survey data.

REFERENCES

Allis, R. G. (1981), "Changes in heat flow associated with exploitation of Wairakei geothermal field, New Zealand," *New Zealand Journal of Geology and Geophysics*, **24**, 1–19.

Allis, R. G., Nash, G. D., Johnson, S. D. (1999), "Conversion of thermal infrared surveys to heat flow: comparisons from Dixie valley, Nevada, and Wairakei, New Zealand" *In:* Transactions Geothermal Resources Council, **23**, 17-20/10/99.

Banwell, C. J., Cooper, E. R., Thompson, G. E. K. and McCree, K. J. (1957), "Physics of the New Zealand thermal area," *Bulletin 123*, DSIR Wellington, New Zealand, 30-36.

Benseman, R. F. (1959), "The calorimetry of steaming ground in thermal areas," *Journal of Geophysical Research*, **64**, 123-126.

Bromley, C. J. and Hochstein, M. P. (2000), "Heat transfer of the Karapiti fumarole field (1946-2000)", *In:* Dunstall, M. G., Morgan, O. E. and Simmons, S. F. (eds.), Proceedings of the 22nd New Zealand Geothermal Workshop 2000, Auckland: University of Auckland, p. 87-92.

Bromley, C. J. and Hochstein, M. P. (2005), "Heat discharge of steaming ground at Karapiti (Wairakei), New Zealand" *In:* Proceedings of the World Geothermal Congress 2005, Antalya, Turkey, 24-29 April 2005.

Dawson, G. B. (1964), **"**The nature and assessment of heat flow from hydrothermal areas," *New Zealand Journal of Geology and Geophysics***, 7,** 155-171.

DSIR report (1988), "Assessment of development effects and reservoir response of Tauhara Geothermal Field." *DSIR report for Waikato Valley Authority*, (Chapter 1).

Ellis, A. J. and Wilson, S. H. (1955), "The heat from the Wairakei–Taupo thermal region calculated from the chloride output," *New Zealand Journal of Science and Technology*, **36**, 622–631.

Fisher, R. G. (1965), "Shallow heat survey of Taupo borough and adjacent country," *New Zealand Journal of Geology and Geophysics*, **8**, 752-771.

Gregg, D. R. (1958), "Natural heat flow from the thermal areas of Taupo sheet district (N 94)," *New Zealand Journal of Geology and Geophysics*, **1**, 65-75.

Hochstein, M. P. and Bromley, C. J. (2005), "Measurement of heat flux from steaming ground," *Geothermics*, **34 (2)**, 131-158.

Hochstein, M.P. and Bromley, C.J. (2001), "Steam cloud characteristics and heat output of fumaroles," *Geothermics*, **30 (5)**, 547-559.

Hunt, T. M., Bromley, C. J., Risk, G. F., Sherburn, S. and Soengkono, S. (2009), "Geophysical investigations of the Wairakei Field," *Geothermics*, **38 (1)**, 86-97.

Mongillo, M. A. (1993), "Atmospheric pressure effects on shallow ground temperatures in geothermal areas: report to the Chief Executive Officer," *IGNS unpublished report*, **#78115**.

Mongillo, M. A. and Graham D.J. (1999), "Quantitative evaluation of airborne video TIR infrared survey imagery," *In*: Proc..21st New Zealand Geothermal Workshop, Univ. Auckland.

O'Sullivan, M. and Yeh, A. (2010), "Wairakei-Tauhara modelling report," Uniservices and University of Auckland, Auckland, New Zealand, p. 283, for Contact Energy.

Thompson, G. E. K., Banwell, C. J., Dawson, G. B. and Dickinson, D. J. (1964), "Prospecting of hydrothermal areas by surface thermal surveys," *In*: Proceedings of the UN Conference on New Sources of Energy (Rome, 1961), **2**, 386-401.

Wildlands, (2004), "Geothermal vegetation of the Waikato Region," Contract Report 896 prepared for Environment Waikato.